WIRELESS FUNCTIONAL OPTICAL IMAGER

by

Serkan Karaca

B.S. in Electronics Engineering, Erciyes University, 2002

Submitted to the Institute of Biomedical Engineering
in partial fulfillment of the requirements
for the degree of
Master of Science
in
Biomedical Engineering

Boğaziçi University
July 2005

WIRELESS FUNCTIONAL OPTICAL IMAGER

APPROVED BY:

Assistant Prof. Dr. Ata Akın (Thesis Supervisor)	.....
Assoc. Prof. Dr. Albert Güveniş	.....
Assoc. Prof. Dr. Mehmed Özkan	.....

DATE OF APPROVAL: 19.08.2005

ACKNOWLEDGMENTS

I would like to thank all the fine people who joined to my life and add a meaning.

These people include my supervisor Dr. Ata Akın. He held my hand from the beginning of my master and never gave up. His guidance, motivation, constant support and understanding are invaluable for me.

I would like to thank Gökhan Işık for his kindness and counseling from the beginning of my master and sharing his deep experience generously, and I would like to thank my home mates Yahya Civelek and Mustafa Küçükkatırcı (MKK) for their constant support and amity for the past 8 years.

I would like to thank Gökhan Ertaş for his critical support while I was in trouble. It is invaluable for me.

I would like to thank my laboratory friends Ömer Şaylı, Uzay Emrah Emir and Murat Tümer for their assistance during my study.

I would like to thank Erhan Uyanık and Bora Büyüksaraç for their assistance in designing the box of the device.

I would like to thank Alper Benli and K. Genç who have no interest in this project.

Last, but not least, I would like to thank my family for everything they do from the beginning of my life.

ABSTRACT

WIRELESS FUNCTIONAL OPTICAL IMAGER

Functional imaging of brain offers the capability to investigate cerebral blood circulation and oxygen metabolism, as well as activity levels of the nervous system. In recent years, technological progress in biophotonics has led to the development of functional near infrared spectroscopy system (fNIRS) which provides non-invasive, rapid and affordable method of monitoring brain oxygenation levels during cognitive activity and even sleep.

This M.Sc. thesis is involved with the development of a prototype of a compact wireless optical imaging system (WFOI). WFOI is composed of a probe that houses inexpensive photodiode detectors (PD), LED working in the near infrared spectrum, a LED driver circuit for constant current supply, a data acquisition unit composed of a microcontroller such as a PIC16F877, a data transmission unit, exploiting the RF communication technology and a PC based software for data logging and analysis. WFOI is designed to be used in sleep apnea studies as well as in pediatric research especially for hyperactive children.

Keywords: Functional optical imaging, functional near infrared spectroscopy, neuroimaging, telemetry.

ÖZET

TELSİZ İŞLEVSEL OPTİK GÖRÜNTÜLEYİCİ

Beynin işlevsel görüntülenmesi, sinir sistemindeki aktivitelerin bir göstergesi olan serebral kan dolaşımı ve oksijen metabolizmasının araştırılmasına olanak sağlar. Son yıllardaki biyofotonik teknolojisindeki ilerleme, bilişsel aktivitelerde ve hatta uykuda bile beynin oksijenlenmesinin görüntülenebildiği invazif olmayan, hızlı ve ucuz bir metot olan yakın kızılötesi spektroskopi sisteminin (fNIRS) geliştirilmesine yol açmıştır.

Bu master tezi küçük ve taşınabilir bir telsiz işlevsel optik görüntüleme sistemi (TİOG) 'nin bir prototipinin geliştirilmesi ile ilgilidir. TİOG, ucuz fotodedektörler ve yakın kızılötesi spektrumda çalışan LED'leri barındıran bir Prob, LED'ler için sabit akım sağlayıcı devre, PIC16F877 gibi bir mikrokontrolörden oluşan veri alma ünitesi, radyo frekansı haberleşme teknolojisini kullanan bir verici ünitesi ve verilerin kaydı ve analiz edilmesi için PC tabanlı bir yazılımdan oluşmaktadır. TİOG, uyku apnesi (uykuda solunum durması) ve pediatri çalışmalarında kullanılabilecek şekilde tasarlanmıştır.

Anahtar Sözcükler: İşlevsel optik görüntüleme, işlevsel yakın kızılötesi spektroskopi, beyin görüntüleme, optik görüntüleme, sinir görüntüleme, telemetri.

TABLE OF CONTENTS

LIST OF FIGURES

LIST OF SYMBOLS

I_o	Incident Light Intensity
I_L	Transmitted Light Intensity
$\varepsilon(\lambda)$	Absorption Coefficient
877_1	PIC16F877 on the Data Acquisition Unit
877_2	PIC16F877 on the RF receiver Module
DET1_730	Voltage on the first detector at 730nm wavelength
R	The concentration difference immediately after ischemia
T1	The time to reach half of the R range after ischemia

LIST OF ABBREVIATIONS

WFOI	Wireless Functional Optical Imager
CW	Continuous Wave
FD	Frequency Domain
TR	Time Resolved
PET	Positron Emission Tomography
fMRI	Functional Magnetic Resonance Imaging
BOLD	Blood Oxygenation Level-Dependent
SPET	Single-Positron Emission Tomography
MEG	Magnetoencephalography
EEG	Electroencephalography
ERP	Event Related Potentials
FOI	Functional Optical Imaging
NIR	Near-Infrared
HbO_2	Oxy-Hemoglobin
Hb	Deoxy-Hemoglobin
LED	Light Emitting Diode
ATP	Adenosine Triphosphate
PC	Personal Computer
RF	Radio Frequency
ADC	Analog to Digital Converter
USART	Universal Synchronous Asynchronous Receiver Transmitter
UART	Universal Asynchronous Receiver Transmitter
IC	Integrated Circuit
ASK	Amplitude Shift Keying
FSK	Frequency Shift Keying
TS	Time Stamp

1. INTRODUCTION

1.1 Motivation and Objectives

Monitoring local oxygenation dynamics with minimal discomfort to subjects presents a major challenge, since only this way it is possible to eliminate the interference to performance (as seen functional MRI). One clinical application where continuous monitoring with minimal confounding elements is in sleep studies where the level of brain oxygenation that can be monitored by fNIRS provides effectiveness of the therapeutic interventions.

A portable Continuous Wave Functional Optical Imaging system has been developed at the Biophotonics Laboratory Biomedical Engineering Institute Boğaziçi University. In this thesis the purpose is to miniaturize the existing one and add wireless communication property in order to make it more compact and mobile to have the patient feel more comfortable allowing streamless data acquisition for reliable analysis. The computer software will be improved to obtain good quality imaging.

1.2 State of Art

Different kinds of fNIRS systems are commercially available. These systems may be classified into three groups according to the methods they use. The methods are Continuous Wave (CW), Frequency Domain (FD) and Time-Resolved (TR). Each of the methods has its own advantages and disadvantages.

1.2.1 Continuous Wave Method

The CW method measures only the intensity of light, is very reliable, but allows for only relative or trend measurements due to the lack of information available about the optical pathlength. To address this problem, in current CW instruments, multiple separations of optodes operating simultaneously are required. This allows for a pathlength correction, but only for a homogeneous tissue. The signal to noise ratio is reasonable with this technique. The depth of tissue which can be measured from the surface is varied typically from 1-3 cm. The CW systems can be made quite compact and portable and even wearable, hence they offer a cost-effective solution to functional optical imaging techniques (approximately $25.000)

Commercially available RUNMAN device developed by NIM Inc., and wearable neuro-imaging device developed during the biomedical optics research program at Drexel University are CW systems which are currently in use [1], [2].

NIRS systems developed by TechEn Inc. offers two CW near-infrared spectroscopy systems: the NIRS 4 System and the NIRS Continuous Wave 32 System. Both of the systems are based on proprietary digital-imaging technologies developed at TechEn, Inc. and clinical research conducted at Massachusetts General Hospital [3].

Also, Dr. D. Boas's group at Harvard Medical School has constructed a continuous wave optical imager.

1.2.2 Time-Resolved Method

The time-resolved technique consists of emitting a very short laser pulse into an absorbing tissue and recording the temporal response (time of flight) of the photons at some distance from the laser source. This method allows for separation of the effects due to absorbance of light from the effects due to scattering of light, using a mathematical approximation that is based on diffusion theory. The time-of-flight

method permits differentiation of one tissue from another. In addition, the scattering component provides useful information. One disadvantage of this technique which still needs to be addressed is the large size (not a portable system), the relatively slow data collection (minutes) and analysis, so that information obtained at bedside is not displayed instantaneously, but rather a few minutes later and the high cost (higher than $200.000).

SoftScan is an optical imaging device for the detection, diagnosis and characterization of breast cancer which is commercially available. It is a time-resolved instrument that employs specially developed low power picosecond diode lasers and fast detectors [4]. Also, a TR instrument is developed in Dr. B. Chance's group. This device employs pulsed laser diodes at 780 nm and 830 nm to perform spatially resolved NIR spectroscopy for monitoring motor cortex activity, as well as performing tomographic breast phantom studies [5].

1.2.3 Frequency Domain Method

The frequency domain method is based on the modulation of a laser light at given frequencies, and allows for correction of the detected signal for the different scattering effects of the fluid and tissue components, using data processing algorithms. In this method pathlength information is directly measured. FD system prices are around $100.000 and due to complexity of the instrumentation they are portable only with wheels.

OxiplexTS is a revolutionary new device allowing the measurement of oxygenated and de-oxygenated hemoglobin concentrations in tissue. FD technique is used and the light is modulated at an RF frequency of 110 MHz. The collected light is measured and processed and the absorption and scattering coefficients of the medium are determined. Figure 1.1 is a measurement taken with the OxiplexTS device [6].

Also, Dr. H. Jiang's group at Dartmouth college has developed an optical imaging device which uses FD technique [7].

1.3 Thesis Contribution

One application of functional optical imaging is in muscle studies. Figure 1.1. shows measurements on human calf muscle during exercise. Changes in hemoglobin oxygenation and concentration can be correlated with various clinical conditions. For example, an increase in oxygenated hemoglobin concentration during exercise accompanied by no change or an increase in de-oxygenated hemoglobin concentration may indicate a venous occlusion which restricts the flow of de-oxygenated hemoglobin out of tissue. Similarly, arterial occlusions may be identified by significant decreases in oxygenated hemoglobin concentrations. The magnitude of hemoglobin changes as well as the rate of change may correlate with the type and extent of vascular disease. A wide variety of tissue oxygenation research is possible.

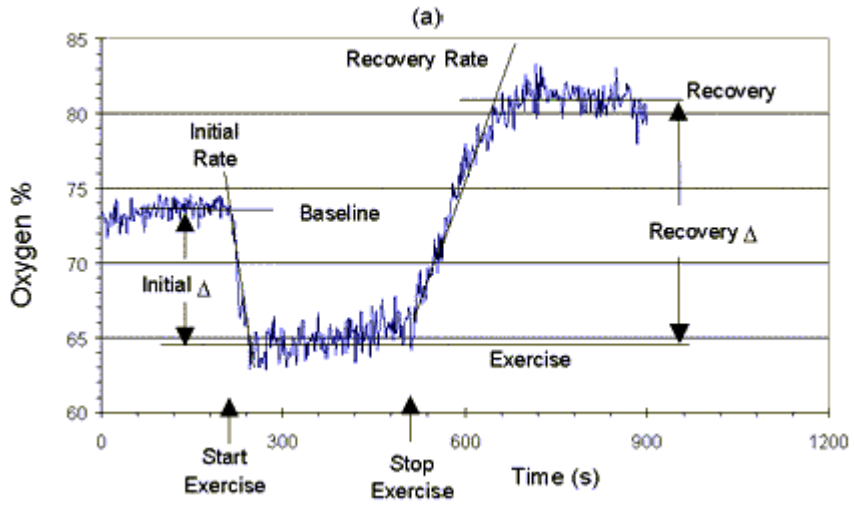

Figure 1.1 Measurements on human calf muscle during exercise.

Figure 1.1. shows the ratio of Oxygenated to Total Hemoglobin Concentration as a percent. Also shown are some of the measurement parameters that can be correlated with physiological conditions including baseline (pre-exercise) value, change as a result

of exercise, rates of change at the beginning and end of exercise, and final value after recovery from exercise.

At this point, usage of wireless technology becomes crucial. Monitoring muscles during exercise and guaranteeing subject's comfort are very important to obtain high quality results. WFOI system is designed to be mobile allowing the subject to move independent from wires.

The major contribution of this thesis is the integration of two innovative techniques in biomedical engineering: fNIRS and telemedicine. We aim to develope a portable wireless fNIRS system that is capable of transmitting optical imaging data to a near by base for continuous data logging and online analysis. The improvements to the previous system which is developed at the Biophotonics Laboratory may be summarized with the following items:

1. being compact, mobile and battery powered,
2. having wireless transmission property to be used in applications such as muscle studies and sleep apnea studies,
3. having a simple UART interface to be used with every computer having a serial port,
4. being able to graphically display real-time data for previewing signal levels.

2. PHYSIOLOGICAL BASIS OF OPTICAL IMAGING

In order to understand causes of neurological disorders and mental illnesses systematic experiments and observations must be done. The methodical study of normal cognitive processes in humans and animals is necessary in understanding these disorders. With the development of invasive and non-invasive functional neuroimaging techniques, new opportunities have been offered for studying the neural control, representation and expression of cognitive functions in the alert, normal human. Both Positron Emission Tomography (PET) and Functional Magnetic Resonance Imaging (fMRI) techniques have been used extensively to investigate cognitive function. Within the last decade, optical neuroimaging has been used for noninvasive imaging of human brain function as well [8].

Functional Optical Imaging is a method that it measures hemoglobin concentration which is an indicator of brain activity.

2.1 Functional Optical Imaging (FOI)

Optical Imaging is a new biomedical imaging technique that uses near infrared light to measure absorption as well as scattering properties of biological tissues. First conceived in the mid-1990s, this method was originally used to image inanimate media and long struggled to overcome problems related to strong scattering of biological materials. But, recent advances in light detection technology have led to numerous studies in areas such as breast cancer detection, brain imaging, and monitoring of rheumatoid arthritis in finger joints. While full clinical acceptance comparable to X-ray, Magnetic Resonance, or Ultrasound imaging has not yet been achieved, first commercial systems are available.

This chapter focuses on brain imaging usage area of FOI just to give the basic principles of this technique.

Optical imaging of the human brain is possible because at certain wavelengths in the near infrared part of the spectrum, penetration of centimeters into tissue is possible. Near-Infrared (NIR) light from approximately 700-950 nm is even more weakly absorbed by tissue than the red wavelengths, so it can be used to measure hemoglobin concentration in the brain, and deduce cerebral blood volume. In addition, oxyhemoglobin (HbO_2) and deoxy-hemoglobin (Hb) have different absorption characteristics, so that changes in blood oxygenation can be measured.

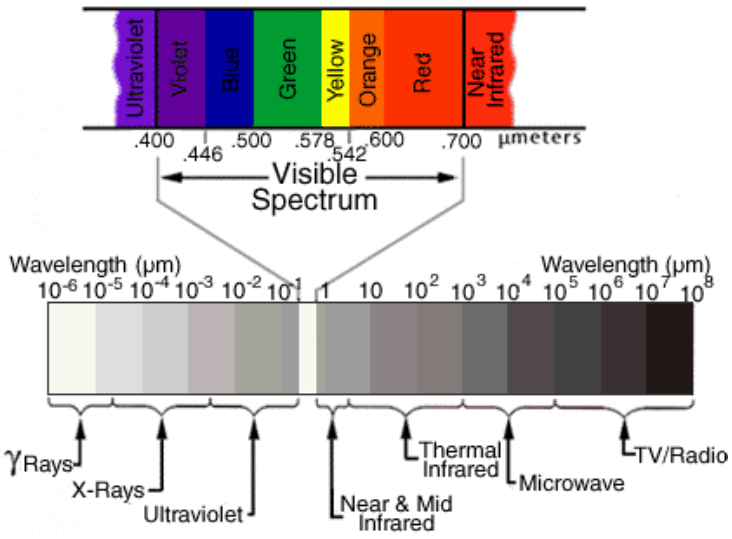

Figure 2.1 Light Spectra.

All of the optical neuroimaging techniques are based on the same model -shine light onto the scalp, detect it as it exits the head, and use the absorption spectra of the light absorbing molecules (chromophores) present in tissue to interpret the detected light levels as changes in chromophore (The chemical group that gives color to a molecule) concentrations. Light traveling from LED optode (optical electrode) to the photodetector optode is scattered, refracted, and reflected forming a banana-shaped path as shown in Figure 2.2.

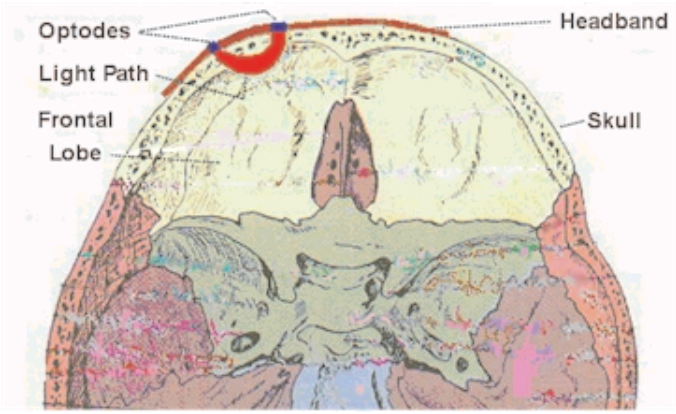

Figure 2.2 Banana-shaped light path between optodes.

The potential advantage of optical over other conventional medical imaging techniques is the unique combination of non-ionising radiation, the potential to differentiate between different types of soft tissue, and the possibility to derive functional information from quantitative measurements of chromophore concentrations [9].

2.1.1 Theory of Operation

In FOI technique, hemoglobin molecule is tracked which gives information about the distribution of oxygen. Let's focus on hemoglobin molecule just to have brief information.

2.1.1.1 Hemoglobin. Hemoglobin is a protein that is carried by red cells in mammals and other animals. It picks up oxygen in the lungs and delivers it to the peripheral tissues to maintain the viability of cells. Hemoglobin is made from two similar proteins that "stick together". Both proteins must be present for the hemoglobin to pick up and release oxygen normally. One of the component proteins is called alpha, the other is beta. Before birth, the beta protein is not expressed. A hemoglobin protein found only during fetal development, called gamma, substitutes up until birth [10].

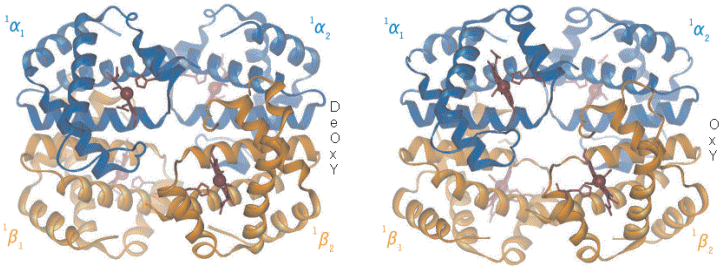

Figure 2.3 Oxy-Hemoglobin (on the left) and Deoxy-Hemoglobin, and alpha (up sides) and beta proteins.

Now, we know hemoglobin is the oxygen carrying molecule in red blood cells. Optical imaging tracks hemoglobin to see where the oxygen is, but why do we need to know the distribution of oxygen in the brain and is this a direct indicator of the activity?

To find an answer we should consider the brain energy metabolism.

2.1.1.2 Metabolism and Blood Flow in the Brain. The brain, like any other organ in the body requires a steady supply of oxygen in order to metabolize glucose to provide energy. This oxygen is supplied by the component of the blood called hemoglobin. The biochemical reactions that transmit neural information via action potentials and neurotransmitters require energy. Glucose, in normal circumstances, is the main energy substrate of the brain [11]. This energy is provided in the form of ATP, which in turn is produced from glucose by oxidative phosphorylation and the Kreb's cycle.

As ATP is hydrolyzed to ADP, energy is given up, which can be used to drive biochemical reactions that require energy. The production of ATP from ADP by oxidative phosphorylation is governed by demand, so that the energy reserves are kept constant. That is to say, the rate of this reaction depends mainly on the level of ADP present. This means that the rate of oxygen consumption by oxidative phosphorylation is a good measure of the rate of use of energy in that area. This oxygen is supplied in the blood. Since oxygen is not very soluble in water, the blood contains the hemoglobin

that oxygen can bind to. When an oxygen molecule binds to hemoglobin, it is said to be oxy-hemoglobin, and when no oxygen is bound it is called deoxy-hemoglobin. The demand for glucose and oxygen by neuronal tissues is responded by the increase in cerebral blood flow to a localized region of brain tissue. The increase in blood flow can be monitored indirectly by measuring the changes in oxy and deoxy-hemoglobin concentrations via FOI (fNIR) method.

So, we know that biochemical reactions that transmit neural information via action potentials and neurotransmitters require energy and this energy is provided in the form of ATP which is produced by oxidative phosphorilation and Kreb's cycle and the oxygen is consumed in these reactions.

At this point, we should understand the theory underlying the operation of tracking hemoglobin molecule by using near-infrared light. This is mostly related to the absorption characteristics of oxy and deoxy-hemoglobin molecules. Let's have a look at the basic principles of absorption.

2.1.1.3 Absorption. Absorbed light is converted to heat or radiated in the form of fluorescence (re-emission of the absorbed light at a longer wavelength). It is also consumed in photobiochemical reactions. Absorption is wavelength dependent and its spectrum depends on the type of predominant absorption centers and water content of tissues. The absorption of light intensity in a non-scattering medium is described by the Beer-Lambert Law. This law states that for an absorbing compound dissolved in a non-absorbing medium:

$$I_L = I_0 \cdot e^{\varepsilon(\lambda)CL} \tag{2.1}$$

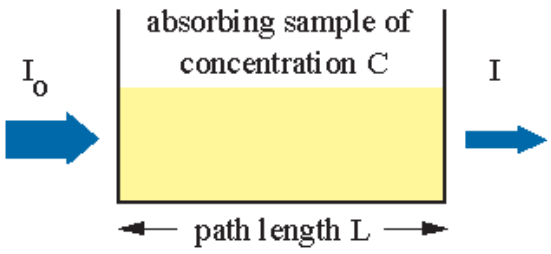

Figure 2.4 Beer-Lambert law.

Where I_0 is the incident light intensity, I_L is the transmitted light intensity through medium, $\varepsilon(\lambda)$ is the absorption coefficient as a function of wavelength, C the concentration of the absorber, and L is the optical pathlength (distance from source to detector) [9]. The equation can be arranged to yield direct information on C, the concentration of the absorber, as:

$$OD(\lambda) = log(I_0/I_L) = \varepsilon(\lambda)CL \tag{2.2}$$

where OD is the optical density.

A compound which absorbs light in the spectral region of interest is known as a chromophore. Each chromophore has its own particular absorption spectrum which describes the level of absorption at each wavelength [12].

Figure 2.5, shows absorption coefficient of oxy and deoxy-hemoglobin molecule at wavelengths 650 nm-1000 nm.

As we see, absorption of Hb and HbO_2 is different in near-infrared spectrum. Only, at the wavelengths approximately 800nm, Hb and HbO_2 absorption is the same and may be used to get information about the total hemoglobin concentration. When we emit light at 730 nm to the scalp and detect it at the end of the path, the signal level at the detector is inversely proportional to the Hb concentration because at this wavelength Hb absorbs light more than HbO_2.

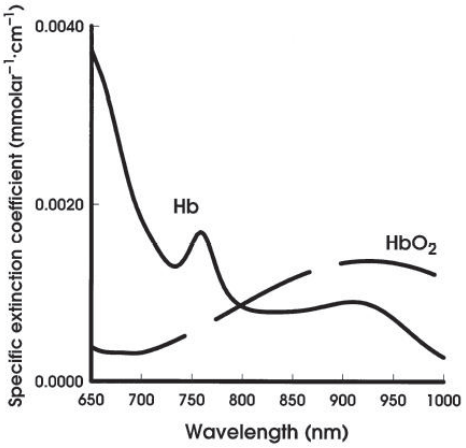

Figure 2.5 Absorption spectrum of oxy and deoxy-hemoglobin.

Beer Lambert law is widely used in chemical spectroscopy, and defines attenuation of light in units of optical density (Eq. 2.2). Attenuation (OD) is measured by comparing the incident light intensity (I_0) against the intensity of the emerging transmitted light (I_L) and expressing this as the number of orders of magnitude that the light intensity has been reduced when traversing the medium.

In order to determine the contribution of multiple chromophores (e.g., oxy and deoxy-hemoglobin), we must take measurements at one or more wavelengths per chromophore to be resolved. For example, by measuring the change in light intensity at two wavelengths, and using the known extinction coefficients of HbO_2 and Hb at those wavelengths (in Figure 2.5), one can then separately determine the concentration changes of HbO_2 and Hb by solving the equations with two unknowns for [Hb] and [HbO_2]. (Eq. 2.3, 2.4). This approach can be generalized to more than two wavelengths.

$$\Delta OD(\lambda_1) = (\varepsilon_{HbO_2}(\lambda_1)\, \Delta[HbO_2] + \varepsilon_{Hb}(\lambda_1)\, \Delta[Hb])\, LB(\lambda_1) \tag{2.3}$$

$$\Delta OD(\lambda_2) = (\varepsilon_{HbO_2}(\lambda_2)\, \Delta[HbO_2] + \varepsilon_{Hb}(\lambda_2)\, \Delta[Hb])\, LB(\lambda_2) \tag{2.4}$$

These equations represent the changes in the total light attenuation signal with respect to extinction coefficients (absorption coefficients) of the corresponding tissues. L is the mean free pathlength and B(λ) is the correction of this pathlength with respect to wavelength. Assuming B(λ_1) = B(λ_2) = B, Δ[HbO_2] and Δ[Hb], the changes in HbO_2 and Hb concentrations can be calculated from equations 2.3 and 2.4 as:

$$\Delta[Hb] = \frac{OD(\lambda_1) - \frac{\varepsilon_{HbO_2}(\lambda_1)}{\varepsilon_{HbO_2}(\lambda_2)}\, OD(\lambda_2)}{LB[\, \varepsilon_{Hb}(\lambda_1) - \varepsilon_{Hb}(\lambda_2)\, \frac{\varepsilon_{HbO_2}(\lambda_1)}{\varepsilon_{HbO_2}(\lambda_2)}\,]} \tag{2.5}$$

$$\Delta[HbO_2] = \frac{OD(\lambda_1) - \frac{\varepsilon_{Hb}(\lambda_1)}{\varepsilon_{Hb}(\lambda_2)}\, OD(\lambda_2)}{LB[\, \varepsilon_{Hb0_2}(\lambda_1) - \varepsilon_{HbO_2}(\lambda_2)\, \frac{\varepsilon_{Hb}(\lambda_1)}{\varepsilon_{Hb}(\lambda_2)}\,]} \tag{2.6}$$

Now, we know the theory underlying non-invasive imaging of the oxygen levels in brain tissue and ready to give an overview to WFOI system.

2.2 Brief Overview to Proposed System

Briefly, WFOI system is designed to use the absorption of near infrared light by the hemoglobin molecule depending on if it is carrying oxygen or not, to draw a kind of map representing, which parts of the frontal lobe of the brain is active during daily activities, to enable brain neuroimaging studies. WFOI system is composed of a probe, data acquisition unit, RF transmitter and receiver, an adapter unit (interface controller) to pass data to serial port of PC and a PC based software for logging and analysis.

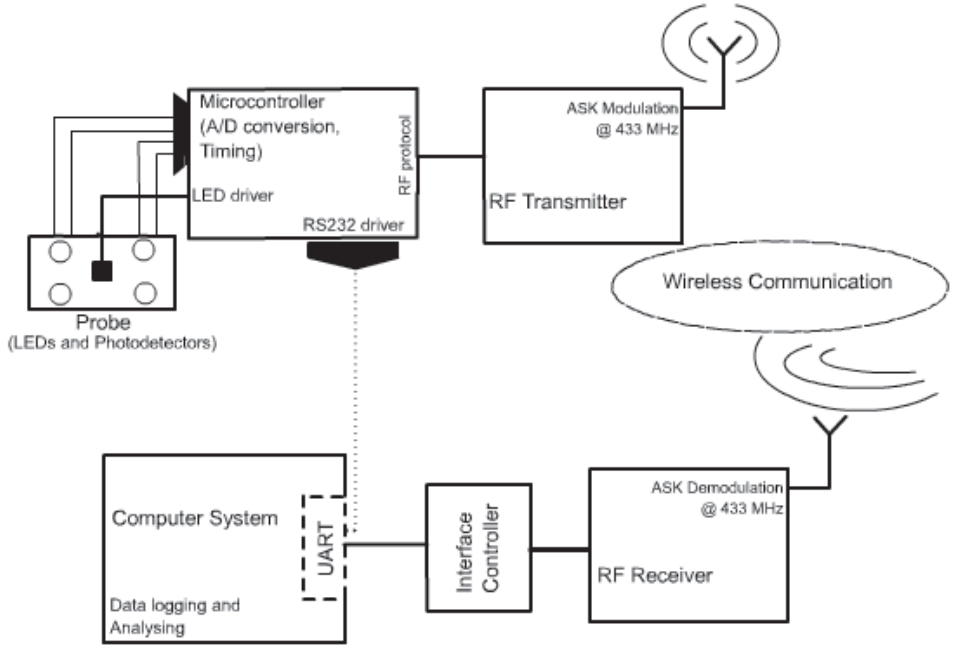

Figure 2.6 Overall System Diagram.

As shown in the Figure 2.6, WFOI system uses a probe which has a LED and Photodedectors on it. LED is used for emitting NIR light to the scalp and photodetectors measures the signal level of reflected and scattered light coming from the tissue.

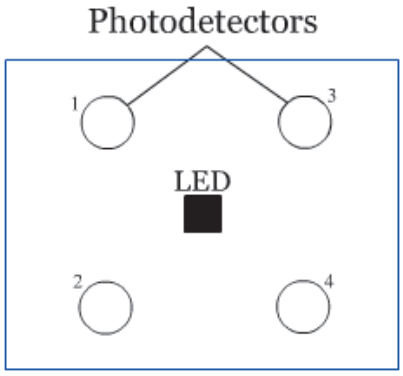

Figure 2.7 The Probe.

LED has multiple wavelengths that emits at 730 nm for Hb and 850 nm for HbO_2. Detectors are sensitive in the NIR spectrum and have high sensitivity for low level signals because light is weakened much while it travels in the tissue from LED to the photodetector (in the Optode).

Detected signals are analog voltages and are converted to digital form in order to be stored in the computer system. For this purpose, a microcontroller is used to control analog to digital conversion, and is also responsible with the timing and the communication with the computer system through two methods.

Figure 2.8 shows the basic timing diagram of the system. LED will be ON at each data collection through detectors 1,2,3,4. Timing is controlled by the microcontroller. Fifty samples are taken with every detector, so 4x50 voltage values are acquired after LED's activation. This data is averaged and stored for a while before sending them to the host.

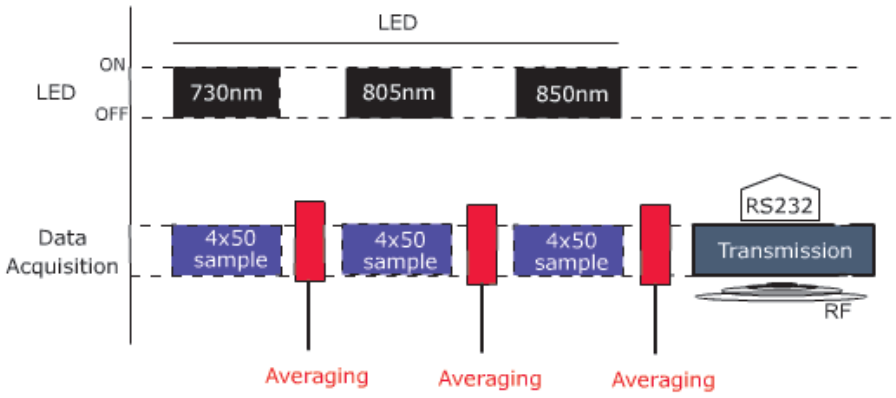

Figure 2.8 Basic Timing Diagram of WFOI.

Before we start to construct the system, there were two choices for wireless transmission one of which was designing our own RF communication transmitter and receiver, and the other one was using an off-the-shelf system. Not to spend much time we decided to use the off-the-shelf system. Bluetooth technology was one of the choices, but the Bluetooth modules and software rights are too expensive due to addition of extra circuitry for security issues such as frequency hopping sequence, encrypted with 128 bits, (options that are not required for WFOI), and it has its own communication protocols. So, we searched for cheaper solutions, like Micrel and Microchip companies' integrated RF devices [13].

We used Microchip's rfPIC12F675 and rfRX0420 as transmitter and receiver and formed our own communication protocol, called Digits protocol which will be explained in the next chapter [14], [15].

For analyzing data at the computer, a software is developed. This software listens to serial port for any data which the system sends, processes it and will have the capability to draw a map representing which optodes are activated more.

3. IMPLEMENTATION OF THE PROTOTYPE

3.1 The Probe

Probe is the most important part of the system. The exact placement where the measurements will be taken plays a crucial role. The anatomical structure of the tissue to be imaged has to be well examined while designing the LED and Photodetector locations. LED-photodetector distance is related to the depth of the tissue where scattered light is coming from. If the distance is increased, deeper parts of the tissue can be scanned.

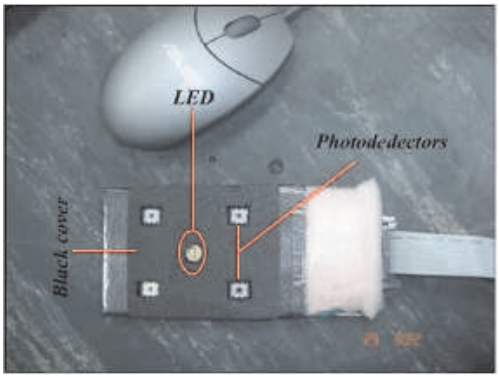

Figure 3.1 The probe.

In muscle studies, it is found using Monte Carlo simulations that mean depth of penetration and lateral spread of light into the tissue is approximately half the source-detector (optode) distance. Monte Carlo is a technique which is used to determine parameters related to the light-tissue interaction such as light path, proportion of the photons arriving to the detector and positioning geometry between tissue and light sources and detectors [16]. Our probe has a LED-detector distance of 2.5 cm, and depth penetration would be 1.25 cm. This is sufficient for an ischemia measurement unless one has thick adipose tissue. In that case, optode distance can be increased [17].

LED and photodetectors are placed on a flexible plastic material and soldered with cables to the probe connector so that probe can be easily fixed on the subject's skin. The probe is connected to the data acquisition unit's connector with a flat cable. For a perfect measure all the detectors and LED must be as close as possible to the skin. No light should be detected from the outside, and no light should be emitted to the space. A black cover is used to fill space between detectors, LED and the skin.

LED emits NIR light at three wavelengths. These are 730 nm, 805 nm and 850 nm. It is EPITEX's multiwavelength LED and typically works with 50mA current. Detectors give output voltages from 0 volt to 5 volts. In general, detected signals from the skin are between 0 and 0.20 volts. So, photodetectors are selected to be sensitive to low-level signals. They are TI's OPT101 Monolithic Photodiode and it has an on-chip single-supply Transimpedance Amplifier making it ideal for battery-operated equipment. It is sensitive to NIR part of the spectrum as shown in the Figure 3.2.

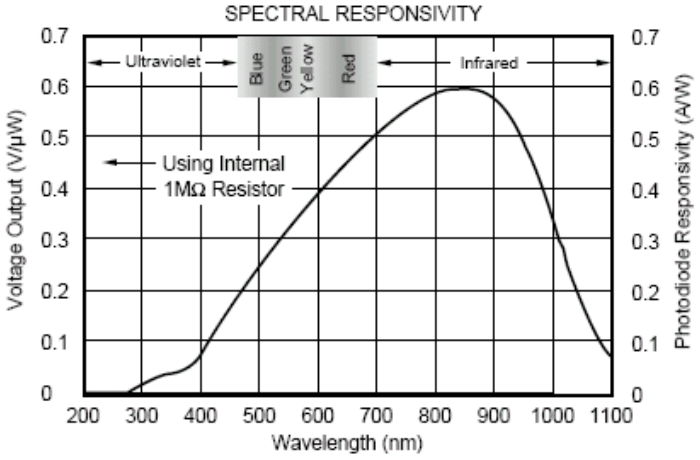

Figure 3.2 Spectral responsivity of OPT101, monolithic photodiode.

3.2 Data Acquisition Unit

Data acquisition unit is composed of the following: A probe connector, a microcontroller, LED driver circuit, an analog multiplexer and a RS232 driver for serial communication.

Probe connector is used to conduct LED current to the probe and get the output signals of the detectors and transmit to the microcontroller to be digitized.

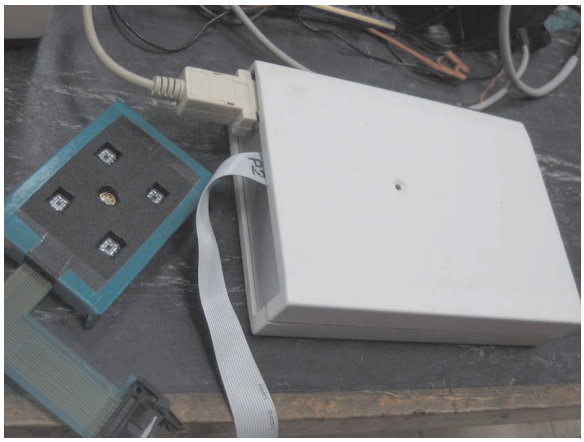

Figure 3.3 Data Acquisition Unit.

Let's explain the other parts.

3.2.1 Microcontroller

Microchip's PIC16F877 microcontroller is used for analog to digital conversion, selection of the LED's wavelength and perform system's timing algorithm, act as a serial interface between the computer which is an optional communication method of the system and implement RF communication protocol algorithms which is called Digits protocol. It is programmed in C language to perform these tasks.

Light levels measured by the detectors are analog voltages and must be converted to the digital form to be stored and analyzed at the computer. PIC16F877's embedded 8 bit, 8 channels ADC is used for this purpose. Channel selection is made by the following C code:

```
set_adc_channel (0);
delay_us(10);

   buff = read_adc();
   DET1_730 = DET1_730 + buff;
```

Figure 3.4 The C code for selecting a channel of the ADC.

With the code in Figure 3.4, first ADC channel is selected and 10s must be waited for the channel to be prepared. Then, converted 8 bit data are read to an integer variable "buff" and stored for a while before transmission in the DET1_730 long integer variable. As we understand from the code, every digitized integer value "buff" is added to the old DETx_730 variable in line 4. This is done for averaging purposes. This code is repeated for every detector for 50 times and total long integer values stored in the variables DET1_730, DET2_730, DET3_730 and DET4_730 are send to the computer. These values are divided to 50 at the computer side and averaging operation is completed.

Averaging operation increases the reliability of the data. This is done for every wavelength. So, 3(wavelength) x 4(detectors) x 50(samples) x 10s = 6ms (approx.) passes until 12 reliable samples from 4 detectors at 3 different wavelengths are prepared for transmission. These samples are 2 bytes values. This means there are approximately 12x2 bytes = 24 bytes of data are transmitted every 7 ms meaning that there must be 3.4 KB/s data rate. Figure 3.5 summarizes the timing algorithm.

As it is said before, there are two ways for the transmission of the acquired data by the microcontroller. One of them is transmission through RS232 protocol and the other is wireless communication.

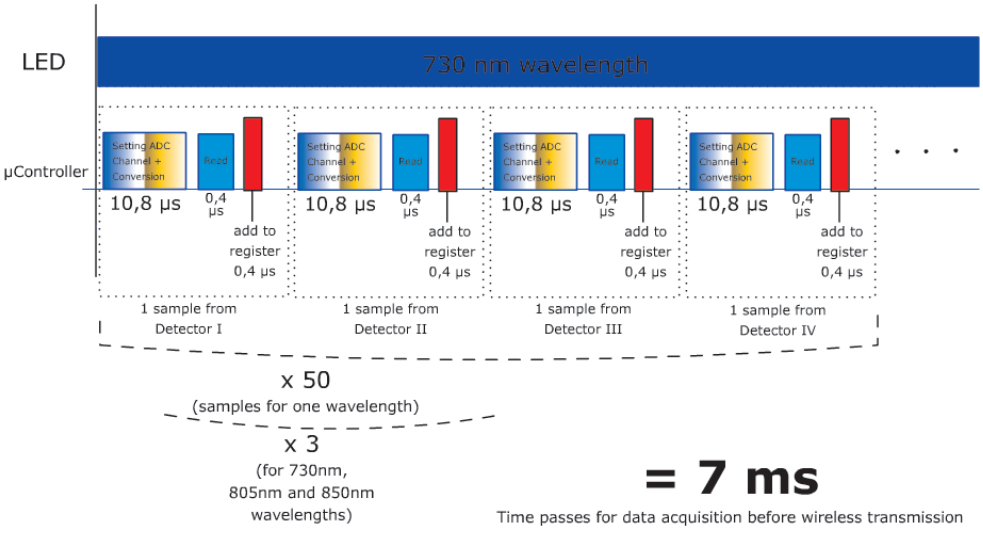

Figure 3.5 Timing diagram of the system.

PIC16F877 has an USART (universal synchronous asynchronous receiver transmitter) interface that helps easily send data to the computer through serial port. Transmission rate can be up to 32 KB/s and this is sufficient for such a system, which requires a data rate up to 3.4KB/s.

3.2.1.1 Synchronous and Asynchronous Communications. There are two basic types of serial communications, synchronous and asynchronous. With synchronous communications, the two devices initially synchronize themselves to each other, and then continually send characters to stay in sync. Even when data are not really being sent, a constant flow of bits allows each device to know where the other is at any given time. That is, each character that is sent is either actual data or an idle character. Synchronous communication allows faster data transfer rates than asynchronous methods, because additional bits to mark the beginning and end of each data byte are not required.

Asynchronous transmission at 19200 baud rate is chosen for WFOI system because it is simple, has sufficient data rate and also requires minimum communication algorithms. Data packages are sent with the form: Startbit - DataBits - Stopbit. Once the start bit has been sent, the transmitter sends the actual data bits. There may

either be 5, 6, 7, or 8 data bits, depending on the number you have selected. Both receiver and the transmitter must agree on the number of data bits, as well as the baud rate. Almost all devices transmit data using either 7 or 8 databits [18].

3.2.1.2 Wireless Communication Protocol. A new communication protocol called Digits protocol is developed for transmission in the air. In this protocol, information is carried in the number of transitions from logic 1s to logic 0s. The digitized voltage values are converted to decimal form and transmitted digit by digit and the digits are separated with the time spaces called SEPARATORs. Number of transitions from logic 1 to logic 0 is proportional to the digit being sent.

For example, A detector voltage of 5 volts is converted to digital form as "11111111" bit sequence by the ADC of the microcontroller. Its decimal form is the number of 255. With digits protocol 255 is separated to its digits as "2", "5" and "5". There is "START" transition sequence meaning that a number is coming through RF transmission, and a "STOP" transition sequence indicates that the number is received. So the package in digits protocol is like:

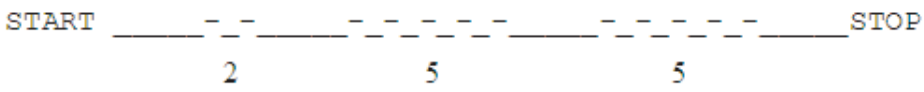

Figure 3.6 A data package in digits protocol (where "-" means logic 1 and "_" means logic 0).

Here, the time spaces between transition sequences are indicating a SEPARATOR and have to be long enough to be detected correctly at the receiver module but also must be short enough not to decrease the transmission speed. Optimum values related to the SEPARATOR duration is being studied.

The purpose of developing a new communication protocol is to be less dependent to the timer modules embedded into the microcontroller. Testing the sensitivity of these modules is a process that requires much time. In conventional 8 bit transmission protocols, complex algorithms have to be constructed for the synchronization issue.

In Digits protocol unnecessary digits of the decimal number is not sent and this reduces the time which has to be spent for the transmission of these unnecessary digits which increases the speed of the transmission.

That is to say, if a voltage value of 0.98 volts is digitized as a bit sequence of "00110010", it's decimal equivalence will be "50" and the digits are "0", "5" and "0". In this protocol, "0" ,most significant digit, is not sent and the data package will be:

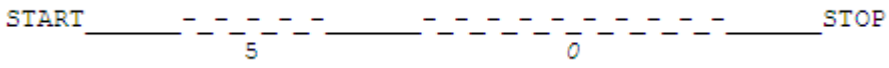

Figure 3.7 A data package in digits protocol.

3.2.2 LED Driver

The light intensity of LED is related to the current passing through it. When drived by a constant voltage source, LED's current decreases or increases if it's resistance changes. In order to hold the current at constant levels using a constant current source is a good way. For these reasons, in WFOI system Burr-Brown's XTR110KP voltage to current converter IC is used. Also its precision internal reference voltage can be used to reduce fluctuations of the current at the output. Two experiments performed to compare the consistency of output currents of this IC and a classic voltage to current converter circuit including a 741 opamp. In these experiments LED's current is observed with the changes in both LED's (therefore the resistance) and ICs' temperature. The procedure of the experiments are as follows:

1. For the first experiment thermometer is connected to the LED and voltage of the circuit is adjusted to give a current of 20mA at the beginning. These voltages are 6,69V for 741 opamp and higher than 13,5V for XTR110KP. After the energy is given to the circuit, LED's temperature and the current through it is measured and saved in a table. This is repeated for every minutes. After 5 minutes, we could obtain a chart showing the changes in LED's current with it's temperature which leds to the change in resistance of the LED. This is a good measure of the performance of the constant current source.

2. In the next experiment thermometer is connected this time to the IC package to measure the temperature of the integrated circuit and same adjustments are performed for a 20mA output from the circuits at the beginning. IC's temperature is increased from 25 C to 50 C degrees with the help of a heater. LED's current is measured and saved in the table for every 5 C increases. This operation gives changes in LED's current with the increasing IC temperature.

3.2.2.1 Experiment Results. These experiments show that XTR110 voltage-to-current converter IC's output current changes less than the classic voltage-to-current converter with 741 opamp circuit's output current with the changes in resistance of the load and the temperature. An increase from 24C to 36C in LED's temperature causes a change in the output current of 3.8mA with UA741 opamp and a little change of 0,005 mA with XTR110 IC. 25 C of change in IC temperatures results with a same response of 0,005 mA with XTR110 and 5,6 mA of change with UA741, and also at the temperature below 35 C degree, minute changes with 741 reaches to 18mA. Table 3.1 and Table 3.2 list all these results related to the comparison of the ICs XTR110 and UA741.

Although the stability of the output current of XTR110 is better, voltage-to-current converter with UA741 is able to produce higher currents up to 100mA, and requires less source voltage. Figure 3.8 shows the basic circuit connection of XTR110. Mosfet used in the circuit is SIEMENS's BUZ171, P channel, enhancement mode MOSFET.

Table 3.1
Experiment 1: Observation of LED's current and temperature during the operation.

Current	**1st min.**		**3rd min.**		**5th min.**		**Max Change in**
Source IC	I(mA)	t.(C)	I(mA)	t.(C)	I(mA)	t.(C)	**LED Current**
UA741	20.3	29.3	21.75	34.7	19.4	36.2	3.8mA
XTR110	19.9	29	19.9	33.7	19.9	35.2	5μA

Table 3.2
Experiment 2: Observation of LED's current while increasing the temperature of the IC.

Current	**IC's Temperature**					**Max Change in**
Source IC	25	30	35	40	45	**LED Current**
UA741	19.4mA	22.98mA	23.68mA	9-25mA	9-25mA	5.6mA
XTR110	19.9mA	19.9mA	19.9mA	19.9mA	19.9mA	5μA

The current consumption of WFOI system changes according to LED's current and it is 30mA when LED current is 20mA and the current through the WFOI system is 47mA when LED's current is 45mA. These have to be taken into consider when designing a compact system.

Because current is directed to the LED through analog multiplexer, its transition time is an important parameter. LED's current have to be rised as fast as possible to the typical values. Maxim's MAX 309 IC, used in the LED driver part has a switching time of 115 ns typical (maximum 450 ns). This is sufficient because there are 10 μs delays for analog to digital converter channel to get ready after every LED's activation.

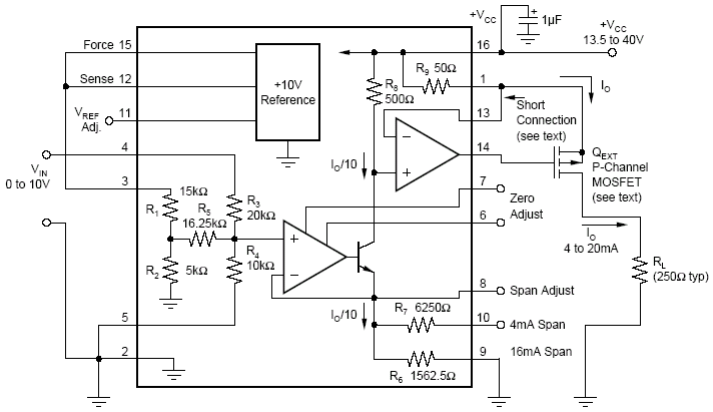

Figure 3.8 Typical application of XTR110 voltage-to-current converter.

3.2.3 RS232 Driver

RS-232 is a serial communications standard that provides asynchronous communication capabilities. The information is sent one bit at a time. Asynchronous tells us that the information is not sent in predefined time slots. Data transfer can start at any given time and it is the task of the receiver to detect when a message starts and ends.

In RS232 standard voltages of -3V to -25V with respect to signal ground are considered logic '1' (the marking condition), whereas voltages of +3V to +25V are considered logic '0' (the spacing condition). The range of voltages between -3V and +3V is considered a transition region for which a signal state is not assigned [18].

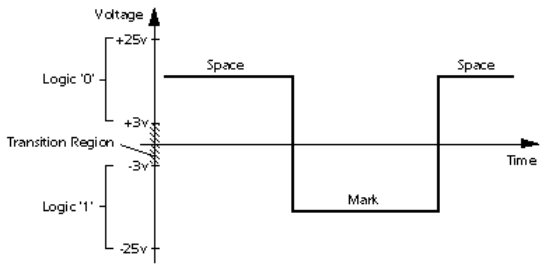

Figure 3.9 Signal State Voltage Assignments in RS232 Standard.

As it is said before, in WFOI system has two optional communication ways. Data at the RF receiver unit and the data acquisition unit is sent to the computer from the serial communications port which uses the RS232 standard. Microcontroller is responsible with this transmission and it is made through the USART interface of PIC16F877. Because of the voltage states in RS232 standard, USART interface voltage states have to be regulated for the RS232 standard in order for the data to be sent to the computer correctly. For this purpose a Maxim's MAX232 RS232 driver IC is used. PIC16F877's USART output is conducted to one of the inputs of MAX232 and the output is conducted to the serial port connector's second pin as shown in the Figure 3.10.

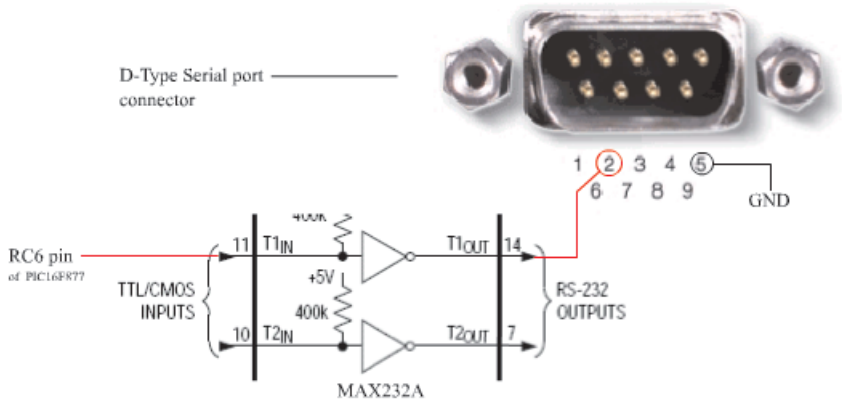

Figure 3.10 Connections between RC6 (16F877's USART interface transmitter pin) and MAX232 (RS232 Driver IC) input, and MAX232 output and Serial Port connector's receive data pin.

3.3 RF Transmitter

For the implementation of the wireless communication protocol, Microchip's rfPIC Development Kit 1 is used. It is a demonstration and development kit for the rfPIC12F675K and rfPIC12F675F PICmicro microcontrollers with UHF ASK/FSK transmitters and rfRXD0420 UHF ASK/FSK/FM receiver. rfPIC12F675F 433.92 MHz transmitter and rfRXD0420 433.92 MHz receiver modules, coming with the rfPIC kit, can be used for discrete applications. We used these modules separately because kit's development board does not give an output which we can use. PIC12F675 in the transmitter module is programmed with a sample transmitter application.

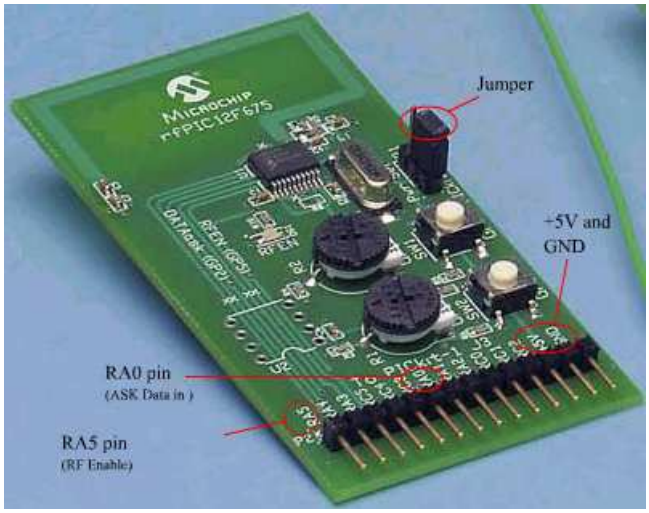

Figure 3.11 rfPIC12F675F 433.92 MHz Transmitter Module.

As shown in the Figure 3.11, RfPIC12F675 Transmitter's ASK data in, RF Enable, Vcc and GND pins are available externally on the module for the user. ASK data in and RF Enable can be used by the pins labeled as RA0 and RA5. For the transmission in WFOI system, ASK Data in pin is connected to 5 volts and bit sequences are transmitted by switching the RA5 pin (RF Enable) ON and OFF by a single BC238 transistor.

The jumper is used for the supply voltage selection. In that position seen in Figure 3.11, the module uses an external supply. RF Transmitter module can also be launched by its own battery by changing the jumper position.

3.4 RF Receiver Unit

Receiver unit consist of a rfRXD0420 433.92 MHz Receiver Module, a second PIC16F877 microcontroller and a MAX232 RS232 driver. The microcontoller in this unit which will be called as "877_2", acts as a serial adapter between RF protocol and USART protocol.

Figure 3.12 rfRXD0420 433.92 MHz Receiver Module.

Receiver module can be controlled by using the pins Vcc, GND and RC1 pin. RC1 pin is the ASK data out pin of the receiver and follows the transitions sent from the transmitter.

RC1 pin, output of the receiver module, is connected to the ADC input of 877_2. 877_2 is programmed to continuously read analog channel and mark a boolean variable "HIGH" as "1" if the voltage at the analog input is higher than 2 volts. START, Data and STOP transition sequences are detected by this algorithm. After the STOP sequence is detected decimal value is calculated by using the digits and a Time Stamp (TS) is sent through RS232 driver to the computer before sending this value with the specific format ([X1]Y1-). TS is calculated by the timers in the 877_2 and used distinguish data coming from the detectors.

Transmitter and receiver modules are able to communicate from distances about 50 meters.

3.5 PC Based Software

The software called Imager in the WFOI system is designed by using Delphi 5 integrated development environment. It is used for logging data that the system acquires, and it has the capability to real-time displaying signal levels at the detectors which are inversely proportional to the hemoglobin concentrations.

Imager, at this state, reads UART buffer every 100 ms and processes any received data to calculate and determine the voltage values, detector and wavelength information and displays the voltages on the interface as shown in the Figure 3.13. Communication with the UART interface is done by a Delphi component called Comport. By this component serial transmission rate and UART buffer size can be adjusted. The buffer can be read by simple "comport1.ReadString" function. In the Imager, com-port component version 2.2 is used. This component can be downloaded from the winsoft company's website [12].

Being in the development process, imager will be able to draw a map which will be a representation of the oxygen distribution under the probe. After, adding the property of two way communication, various adjustments will be made from the software by means of sending commands to the microcontroller at the data acquisition unit.

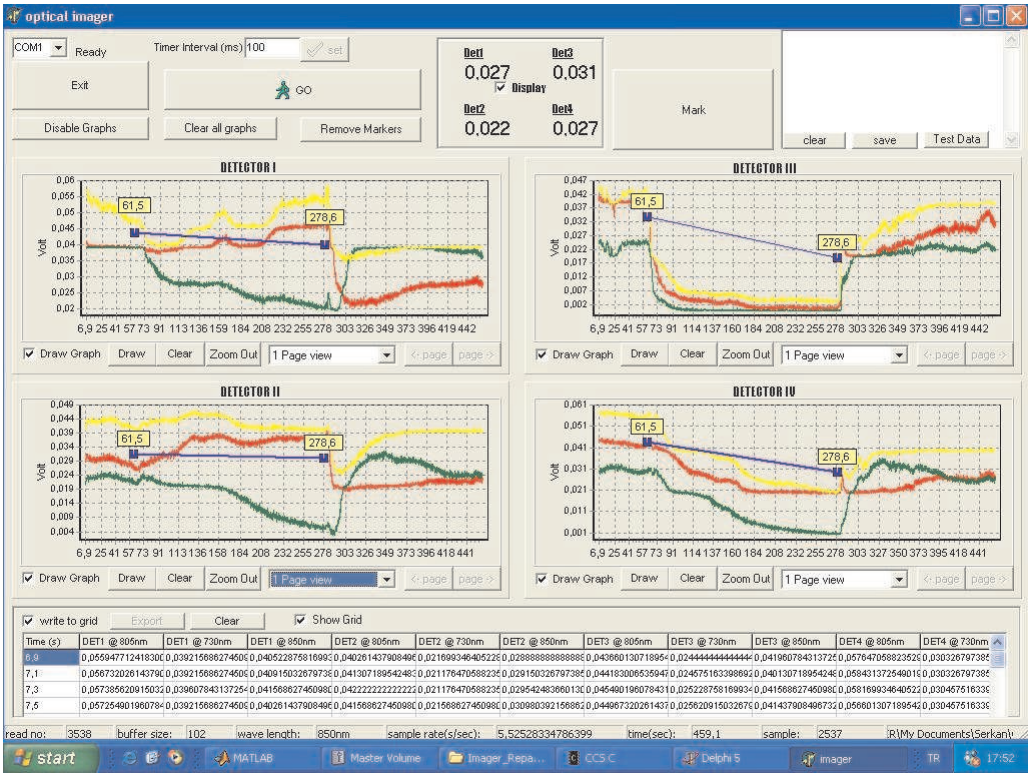

Figure 3.13 A screenshot from the Imager during an ischemia measurement.

Imager displays voltage levels in three forms: a digital display at the top to show the instant voltage values at the detectors, graphical display at the center and a table display at the bottom. Data on the graphical displays can be saved in the form of a bitmap file and the content of the table can be saved in a text file for further analysis with different programs like MATLAB.

For the validation of NIRS measurements ischemia protocol is an important method in which the blood flow (and thus oxygen) is restricted to a part of the body. Figure 3.13 is a screenshot taken after an ischemia measurement. Green lines indicate the light intensities in 730nm of light (yellow line is used for 805 nm, and red line is used for 850 nm). Y axis represents the voltage levels in volts and X axis represents the time in seconds. Blue lines and the corresponding time stamps can be putted by the "Mark" button to show the beginning and the end of the experiment. Here, they indicate the start of the restriction of blood flow to the upper arm by using a cuff, and the release of it. We used equations 2.5 and 2.6 derived from Beer Lambert law in MATLAB environment to calculate the changes in Hb and HbO_2 concentrations from data acquired with the system.

3.5.1 Validation Process

For validating the system, we used two types of measurement protocols. These are ischemia measurement and muscle exercise for investigating the oxidative metabolism of the working human muscle under ischemic conditions.

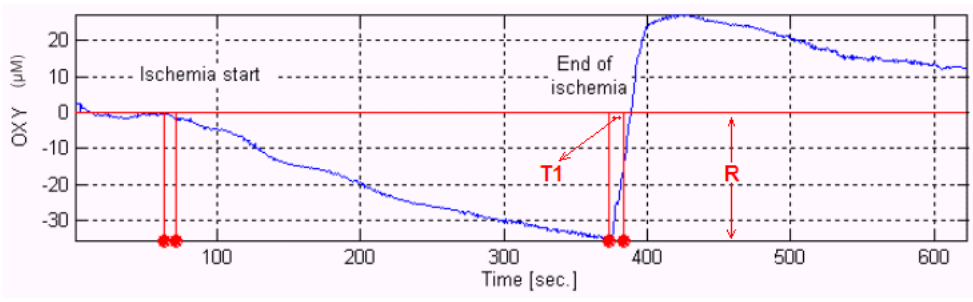

Figure 3.14 Typical trend of [HbO_2] signal in ischemia protocol.

In a typical ischemia measurement, during ischemia [Hb] increases (reaching maximum value) while [HbO_2] decreases (reaching minimum values). Immediately after the ischemia (by lowering the cuff pressure to 0 mmHg), [Hb] decreases sharply, [HbO_2] signal increases (Figure 3.14). These rapid responses are followed by trends returning to the baselines. The concentration difference immediately after ischemia is called range (R) and the time to reach half of this range after ischemia is called half time (T1=2) which gives information about the recovery speed of the probed muscle tissue investigated. This parameter is used for evaluating oxidative metabolism in muscles of different subjects [19].

In muscle exercise protocol, subjects were asked to perform an isotonic forearm exercise that basically consisted of pulling a constant load with their fingers at a frequency of 0.5 Hz. The detectors of the NIRS device were placed on the right forearm and Hb and HbO_2 signals were recorded on the finger joint flexors. All these exercises were performed under ischemic conditions.

After placing the probe on the right forearm of subjects, thirty seconds of rest period is waited. Then 230 mmHg of cuff ischemia is applied to cut the blood flow. When the blood flow is fully cut down, ten seconds of delay period is waited. After ten seconds of delay, finally subjects starts to perform an isotonic forearm exercise by pulling a constant load of 1850 gr. 10 cm. up and down.

Measurements are taken from 2 subjects for the ischemia protocol and 3 subjects for the muscle exercise protocol by using the devices NIROXCOPE 201 (which was developed previously at the Biophotonics Laboratory) and WFOI. Similarities in signal trends are examined.

Figures 3.15 and 3.16 show ischemia measurements and Figures 3.17 and 3.18 show muscle exercise measurements taken from the same subject with both devices. As seen, Hb and HbO_2 signal trends resembles each other.

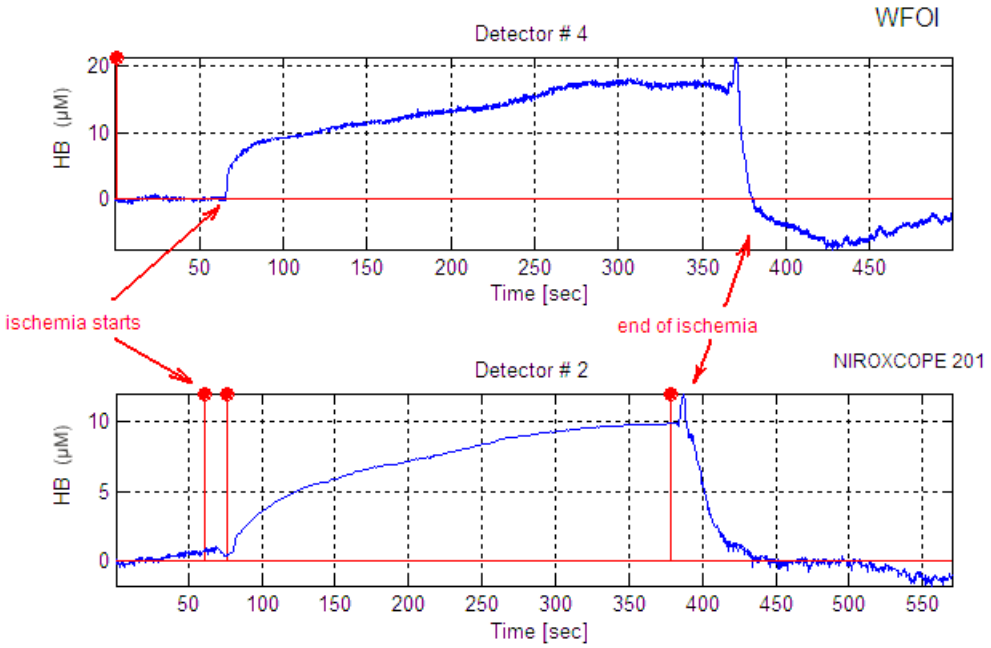

Figure 3.15 Hb trends during ischemia measurements taken with WFOI (upper) and NIROXCOPE 201 from the same subject.

To evaluate the results of data acquired with both devices, also T1 parameter is taken into account. T1, which is related to the recovery speed of the muscle tissue, is calculated for every subject and the difference in this parameter between data acquired with both devices for the same subject is calculated. Results are reported in Table 3.3.

As seen from the results, T1 values calculated from acquired data with both devices are nearly same. The difference in T1 parameters is less than 4 seconds, and is mostly related to the physiological state of the subject and basal metabolism which even varies throughout a day. All of the ischemia and muscle exercise protocol measurement results for each subject can be seen at the appendix.

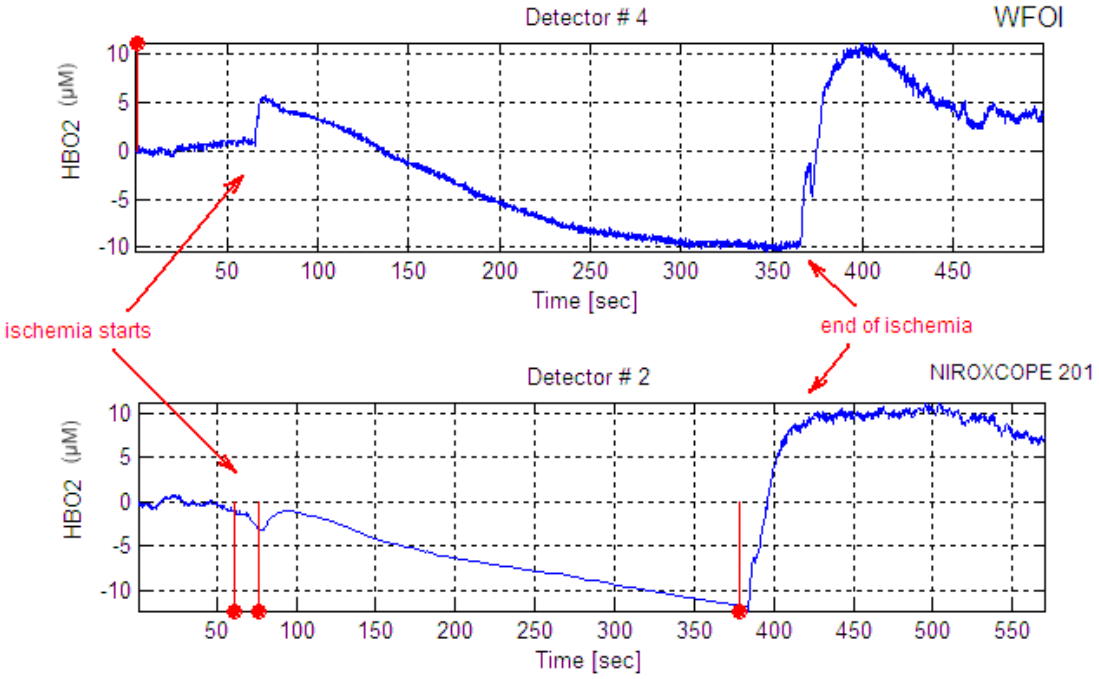

Figure 3.16 HbO_2 trends during ischemia measurements taken with WFOI (upper) and NIROXCOPE 201 from the same subject.

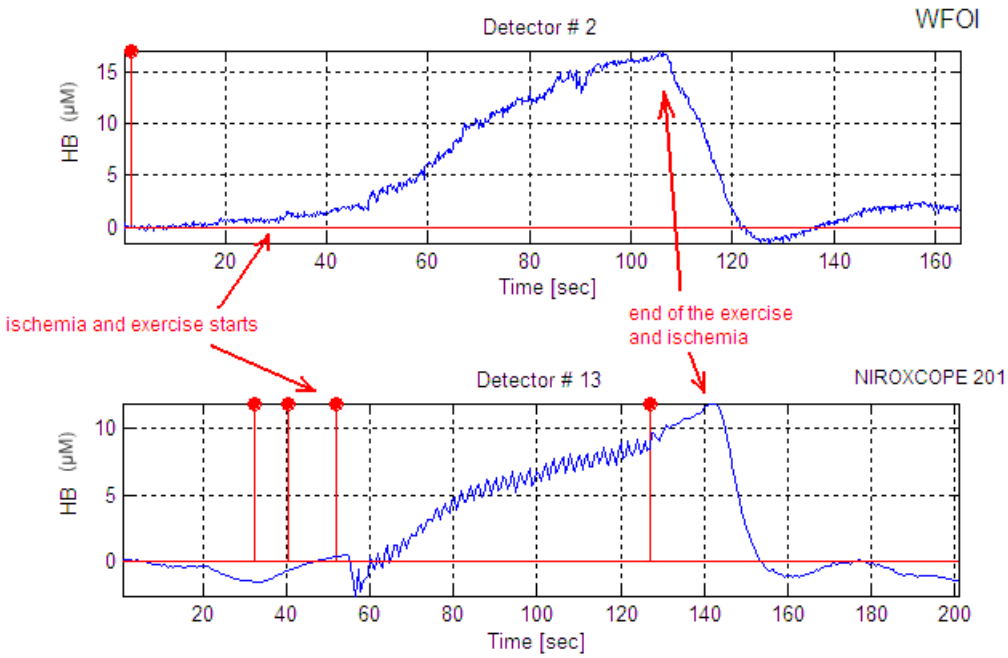

Figure 3.17 Hb trends during muscle oxidative metabolism measurements taken with WFOI (upper) and NIROXCOPE 201 from the same subject.

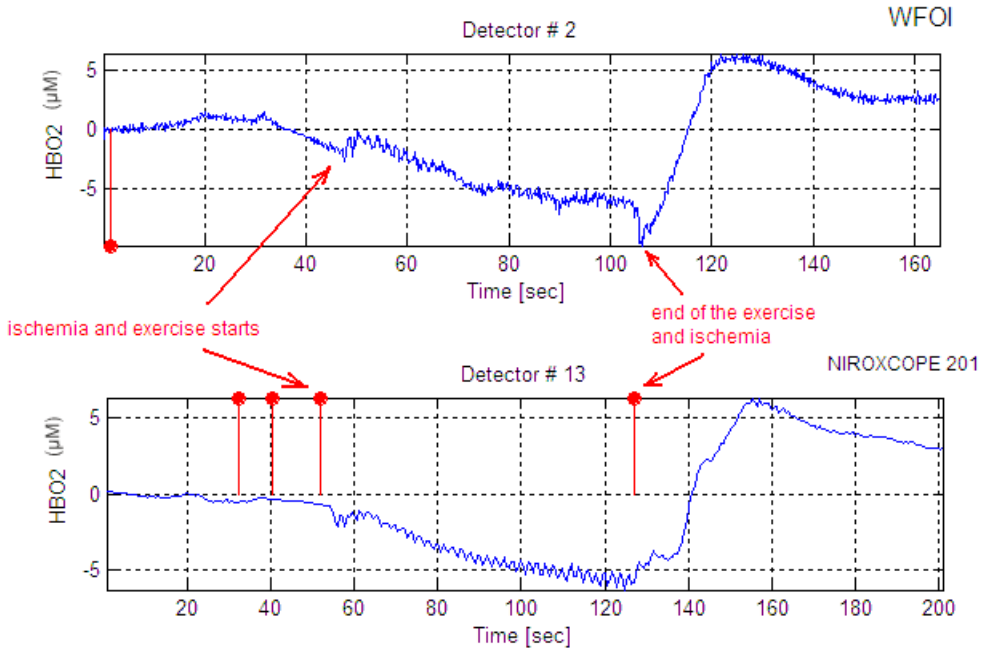

Figure 3.18 HbO_2 trends during muscle oxidative metabolism measurements taken with WFOI (upper) and NIROXCOPE 201 from the same subject.

Table 3.3
T1 values calculated from the data acquired by the devices WFOI and NIROXCOPE 201.

Measurement Protocol	**Subject Index**	**T1 parameter for the device**		**Difference in T1 parameters**
		WFOI	NIROXCOPE 201	
Ischemia	1	15 s	17 s	2 s
Ischemia	2	22 s	25 s	3 s
Muscle Exercise	3	9 s	11 s	2 s
Muscle Exercise	4	9 s	6 s	3 s
Muscle Exercise	5	4 s	5 s	1 s

4. CONCLUSIONS

We aim to develope a wireless FOI system capable of acquiring 140 samples per second if we neglect the delays arising from the transmission and the processing of the software algorithms. Knowing that the hemodynamic signals change slowly this data rate is sufficient for real-time imaging. As seen in the Figure 2.5, the values obtained by the addition of 50 samples taken from every detector at one wavelength (for example 730 nm) is prepared for transmission at 7 ms. Table 4.1 lists the specifications of WFOI system.

Table 4.1
Specifications of the system.

Method of operation	Continuous Wave (CW)
Measurements	Oxy- and deoxy-hemoglobin concentration Total hemoglobin concentration
Light sources	Multiwavelength LED (730, 805 and 850nm)
Light detectors	Monolithic Photodiode
Average optical power	Less than 1 mW
Total number of measurement channels	Four
Spatial resolution	4 Emitter-Detector distances
Data acquisition rate	From 40 ms to minutes
Maximum experiment duration	2 hours (approx.)
Connection to computer	Serial Port
Software operating system	Windows 98/2000/XP
Dimensions and weight	18 x 14 x 4 cm, 200 gr
Electrical power requirements	2 x 9V battery

The following items are used during the construction of the WFOI system:

1. LED (Epitex).
2. Photodetector (OPT101 - TI).

3. Microcontroller (PIC16F877 - Microchip).
4. RS232 Driver (MAX232 - Maxim).
5. Analog Multiplexer and switches (MAX309 and MAX333 - Maxim).
6. Precision Voltage-to-current converter (XTR110KP - Burr Brown).
7. P channel MOSFET (BUZ171 - Siemens).
8. 8. Microchip rfPIC Development Kit's rfPIC12F675 UHF ASK/FSK transmitter and rfRXD0420 UHF ASK/FSK/FM receiver.

WFOI system has the potential to be used in variety of research areas. Such as:

1. Effects of exercise on muscle for the diagnosis of Peripheral Vascular Disease (PVD).
2. Scanning of the muscle for the location of vascular occlusions.
3. Effects of pharmaceuticals and/or anesthetic gas mixtures on tissue and/or brain.
4. Monitoring of brain oxygenation during surgery.
5. Monitoring of neonatal infant brain oxygenation.
6. Monitoring oxygenation and hemoglobin concentration status of cancer tumors.
7. Monitoring cognitive activity.
8. Monitoring of changes in blood oxygenation and blood volume related to human brain function.
9. Neurorehabilitation studies.
10. Deception monitoring.
11. Muscle monitoring for performance of athletes.

4.1 Future Work

Future work may focus on the probe design. To observe different parts of the body, LED-detector distances must be adjustable. A rail mechanism may be constructed on the probe to change the optode distances easily for different kind of measurements.

Using more detectors in the probe increases the resolution of the image, and filters may be used to prevent visible light from detection by the photodetectors which causes erroneous measurements because, in some cases, black cover can not be able to stop the visible light.

Interface of the software may be improved to show concentrations of Hb and HbO_2 in graphical form. After adding two way communication to the system, software will have the ability to control data acquisition unit by sending commands to the microcontroller.

Wireless communication protocol may be optimized to increase the transfer speed of data by minimizing the durations of logic 1 and logic 0.

PCB design may be enhanced to reduce the data acquisition unit to be more compact.

APPENDIX A. RESULTS OF THE MEASUREMENTS TAKEN WITH DEVICES WFOI AND NIROXCOPE 201 FOR A COMPARISON AND EVALUATION

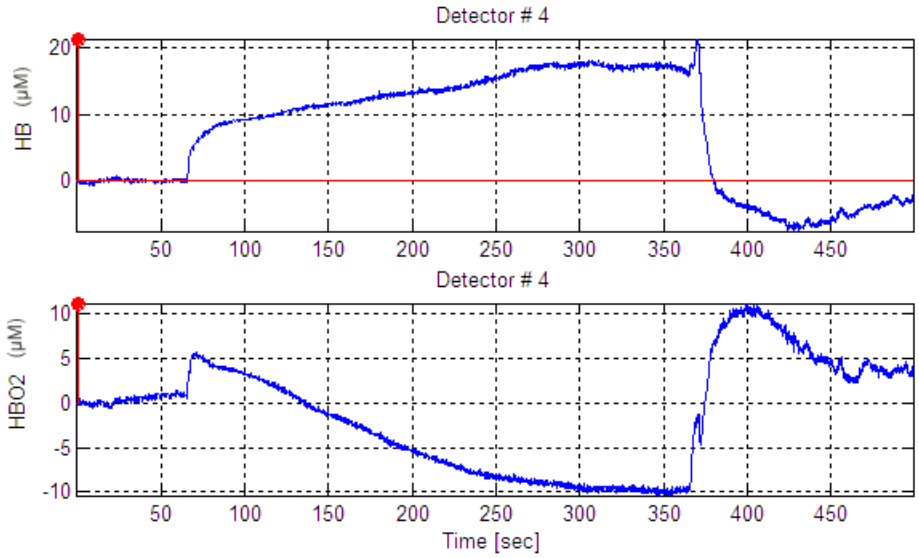

Figure A.1 Hb and HbO_2 trends during an ischemia measurement taken with WFOI system from subject 1.

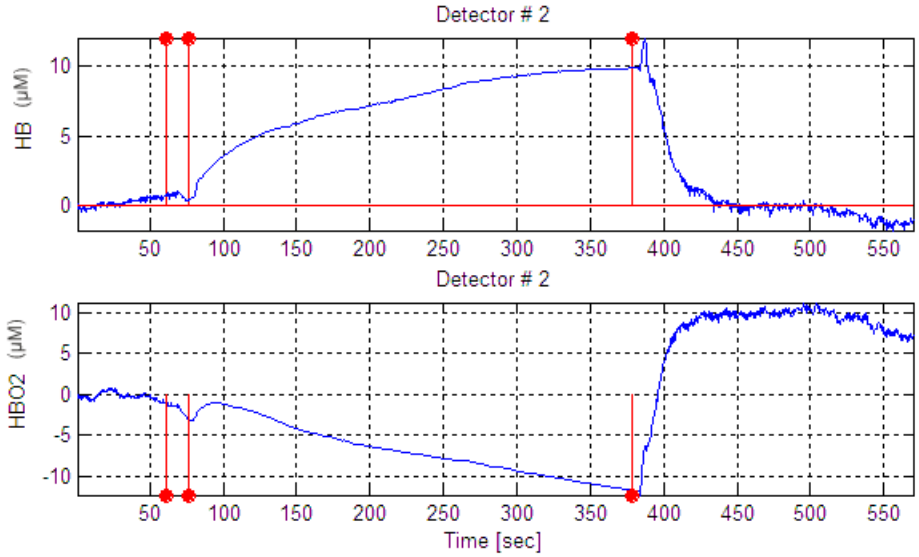

Figure A.2 Hb and HbO_2 trends during an ischemia measurement taken with NIROXCOPE 201 from subject 1.

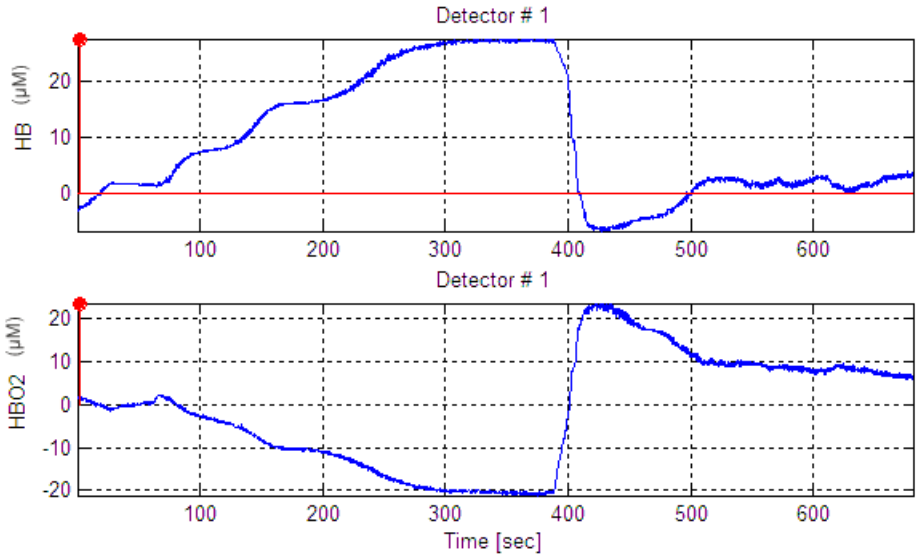

Figure A.3 Hb and HbO_2 trends during an ischemia measurement taken with WFOI system from subject 2.

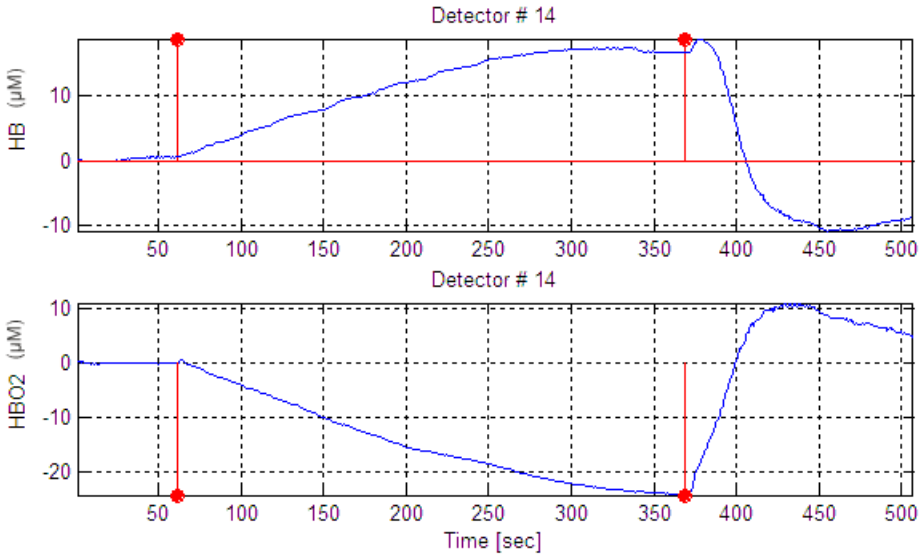

Figure A.4 Hb and HbO_2 trends during an ischemia measurement taken with NIROXCOPE 201 from subject 2.

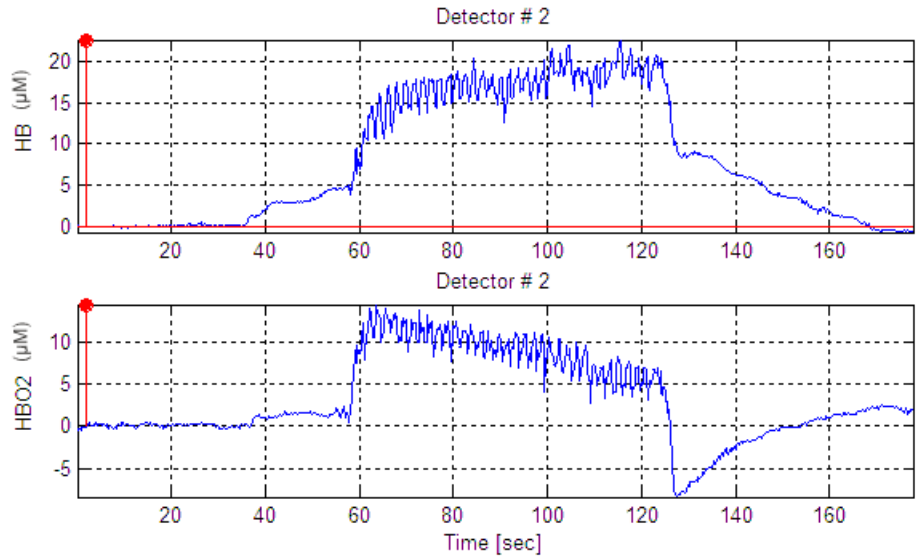

Figure A.5 Hb and HbO_2 trends during a muscle exercise measurement taken with WFOI system from subject 3.

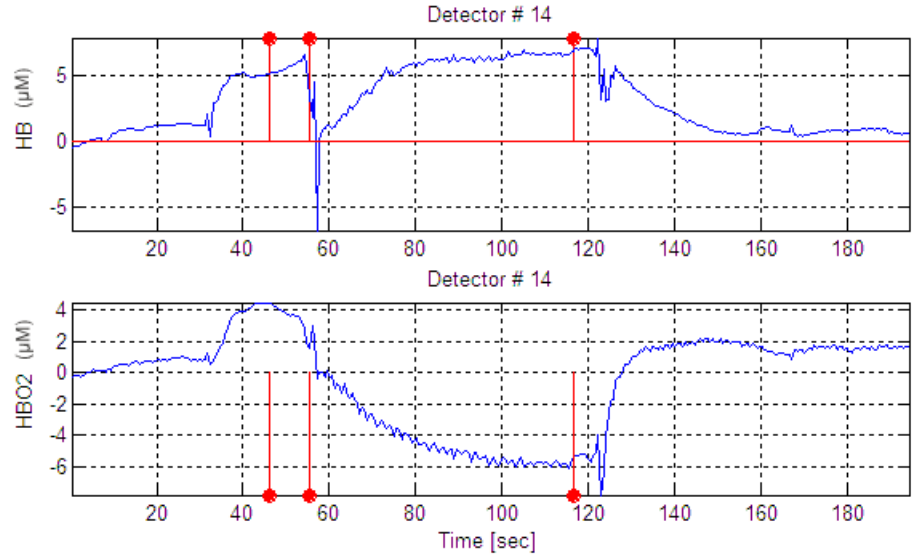

Figure A.6 Hb and HbO_2 trends during a muscle exercise measurement taken with NIROXCOPE 201 from subject 3.

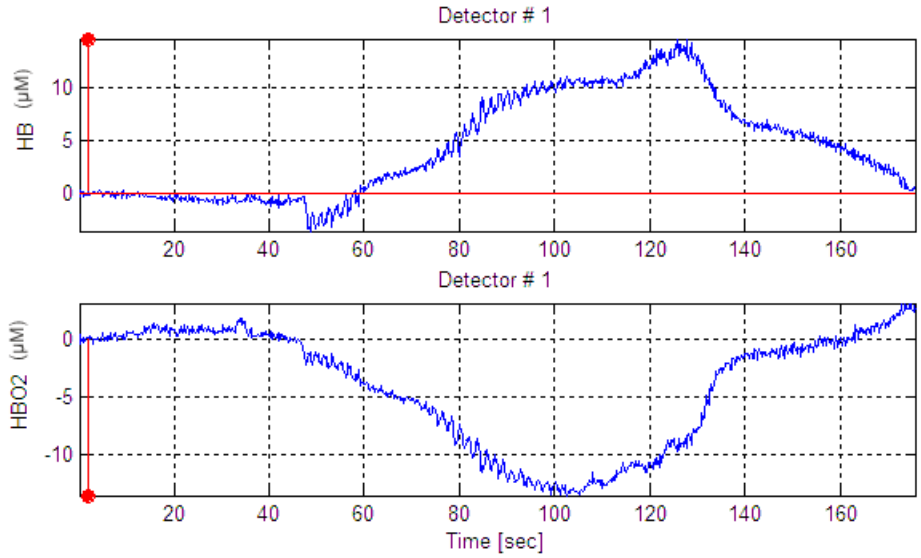

Figure A.7 Hb and HbO_2 trends during a muscle exercise measurement taken with WFOI system from subject 4.

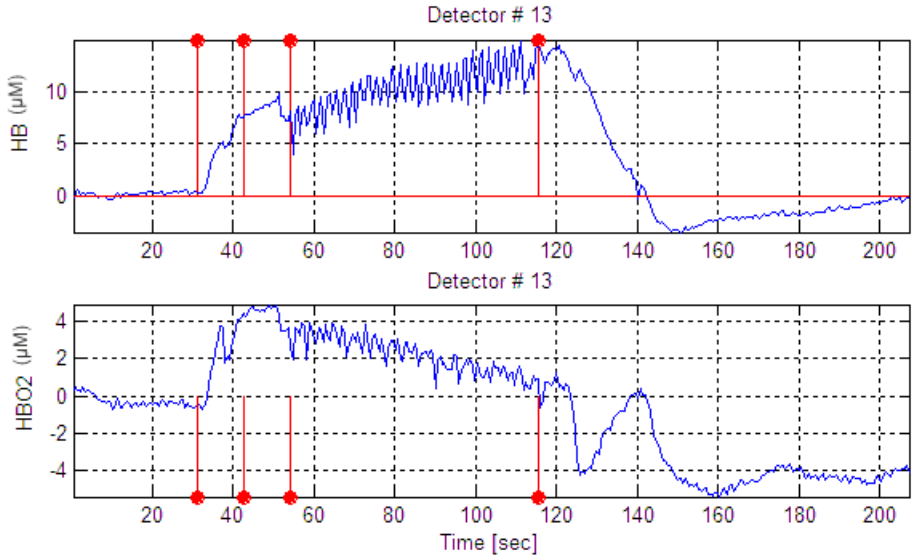

Figure A.8 Hb and HbO_2 trends during a muscle exercise measurement taken with NIROXCOPE 201 from subject 4.

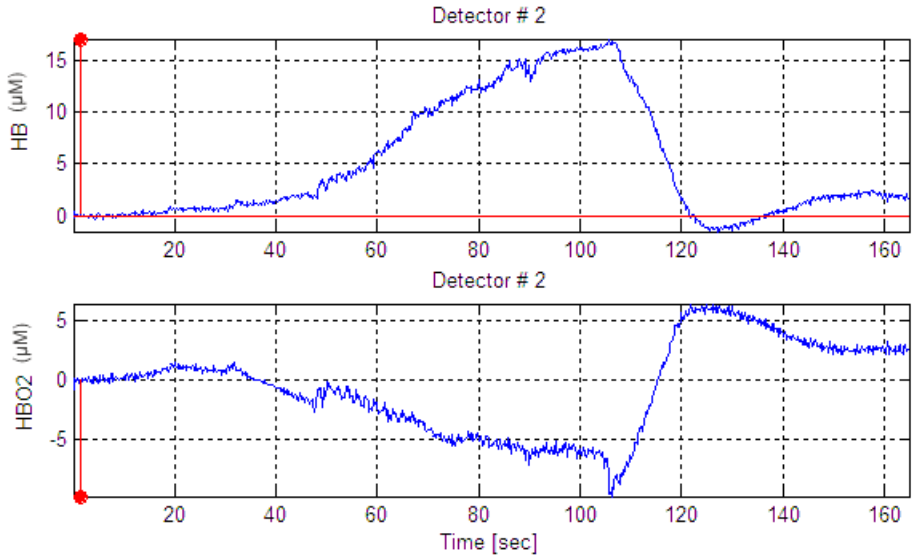

Figure A.9 Hb and HbO_2 trends during a muscle exercise measurement taken with WFOI system from subject 5.

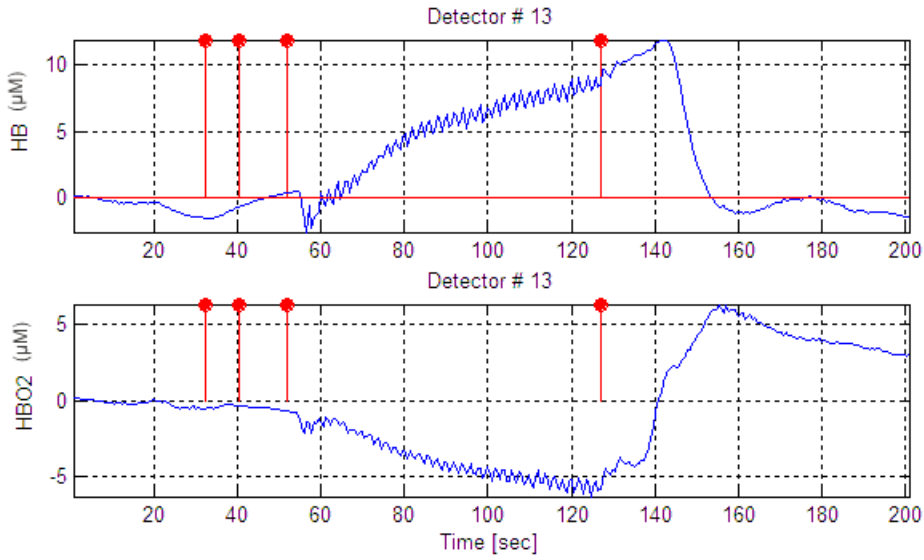

Figure A.10 Hb and HbO_2 trends during a muscle exercise measurement taken with NIROXCOPE 201 from subject 5.

REFERENCES

1. J Patrick Neary, Donald C McKenzie, Y. N. B., "Muscle oxygenation trends after tapering in trained cyclists," *Dynamic Medicine*, Vol. 4, no. 4, pp. 1–9, 2005.
2. http://www.biomed.drexel.edu/ResearchPort/Contents/Biomedical_Optics/.
3. http://www.nirsoptix.com/systems.htm.
4. http://www.art.ca/en/products/softscan.html.
5. http://www.biomed.drexel.edu/ResearchPort/Contents/Biomedical_Optics/.
6. http://www.iss.com/Products/oxiplex.html.
7. Huabei Jiang, Keith D. Paulsen, U. L. O., "Simultaneous reconstruction of optical absorption and scattering maps in turbid media from near-infrared frequency-domain data," *Optics Letters*, Vol. 20, no. 20, pp. 2128–2130, 1995.
8. Emir, U. E., "System characterization of a fast optical imaging," Master's thesis, Boğaziçi University, 2003.
9. Gary Strangman, Joseph P. Culver, D. B., "A quantitative comparison of simultaneous bold fmri and nirs recordings during functional brain activation," *NeuroImage*, Vol. 17, pp. 719–731, 2002.
10. http://sickle.bwh.harvard.edu/hemoglobin.html.
11. Magistretti, P. J., "Cellular mechanisms of brain energy metabolism and their relevance to functional brain imaging," *Phil. Trans. R. Soc. Lond. B*, Vol. 354, pp. 1155–1163, 1999.
12. Chance, B., M. Cope, E. Gratton, N. Ramanujam, and B. Tromberg, "Phase measurements of light absorption and scatter in human tissue," *Rev. Sci. Instru.*, Vol. 69, no. 10, pp. 3457–3481, 1998.
13. www.clarinox.com.
14. www.micrel.com.

15. www.microchip.com.

16. Wang, L. H., and S. L. Jacques, *Monte Carlo Modeling of Light Transport in Multi-layered Tissues in Standard C.* MCML computer program, 1998.

17. Chance, B., M. Dait, C. Zhang, T. Hamaoka, and F. Hagerman, "Recovery from exercise induced desaturation in the quadriceps muscles of elite competitive rowers," *Am. J Physiol.*, Vol. 262, pp. 766–775, 1992.

18. http://www.camiresearch.com/Data_Com_Basics.

19. Ding, H., G. Wang, W. Lei, R. Wang, L. Huang, Q. Xia, and J. Wu, "Non-invasive quantitative assessment of oxidative metabolism in quadriceps muscles by near infrared spectroscopy," *Br. J. Sports Med.*, Vol. 35, no. 6, pp. 441–444, 2001.